Rosenberg, J. M., Khallai, O. B., Kopka, M. L., Dickerson, R. E. & Riggs, A. D. (1977) *Nucleic Acids Res. 4*, 567–572.
Rowe, E. S., & Tanford, C. (1973) *Biochemistry 12*, 4822–4827.
Schnarr, M., & Maurizot, J. C. (1980) *Biopolymers 19*, 1975–1981.
Tanford, C. (1970) *Adv. Protein Chem. 24*, 1–95.
Wade-Jardetzky, N., Bray, R. P., Conover, W. W., Jardetzky, O., Geisler, N., & Weber, K. (1979) *J. Mol. Biol. 128*, 259–264.
Zetina, C. R., & Goldberg, M. E. (1980) *J. Biol. Chem. 255*, 4381–4385.

Nuclear Magnetic Resonance Study of Dihydrofolate Reductase Labeled with [γ-^{13}C]Tryptophan†

John P. Groff,‡ Robert E. London, Lennie Cocco, and Raymond L. Blakley*

ABSTRACT: Dihydrofolate reductase isozyme 2 of *Streptococcus faecium* has been labeled with ^{13}C in the C_γ position of tryptophan residues by growing the organism on a defined medium containing L-[γ-^{13}C]tryptophan (90% ^{13}C). The ^{13}C nuclear magnetic resonance (NMR) spectrum of the enzyme shows four well-resolved resonances which have nuclear Overhauser enhancements of 1.1–1.3. Values of T_1 (spin–lattice relaxation time) and T_2 (spin–spin relaxation time) are significantly less than predicted for an isotropically rotating, rigid sphere with no intermolecular dipole–dipole interactions. Three of the resonances have chemical shifts downfield from the ^{13}C resonance of urea-denatured enzyme by amounts up to 1.43 ppm. The chemical shift of resonance 4 in the spectrum is 4.0 ppm upfield from Trp C_γ of urea-denatured enzyme. This large upfield shift is attributed to electric field effects generated by polar side chains. The two more upfield peaks both provide evidence that the corresponding tryptophan residues, W_C and W_D, each undergo chemical exchange between alternative microenvironments. In the case of W_C, which gives a resonance with two components, exchange is slow (ν_e, exchange rate $\ll 55$ s^{-1}), and the relative populations of the two stable states are in the ratio 2:3. W_D is apparently in intermediate to fast exchange on the NMR time scale. With a two-state model, ν_e increases from approximately 90 to 150 s^{-1} as the temperature is increased from 5 to 25 °C. This increase in temperature is also accompanied by an increase in the fractional population of the minor downfield state(s), from about 0.062 at 5 °C to 0.24 at 25 °C. However, the data may also be interpreted as a temperature-dependent equilibrium between a continuum of many states. W_D is tentatively identified with Trp-22 since comparison of the sequences of *Lactobacillus casei* dihydrofolate reductase and *S. faecium* dihydrofolate reductase and inspection of the crystal structure of the *L. casei* enzyme indicate that Trp-6, Trp-115, and Trp-160 are probably all involved in regions of β sheet whereas Trp-22 is in a loop joining βA to αB. Earlier crystallographic evidence for the *Escherichia coli* reductase suggests that in the methotrexate complex with this enzyme the corresponding loop has a good deal of flexibility. It is probable that in the uncomplexed *S. faecium* reductase the motion of this loop is the major mechanism for the exchange process involving Trp-22. The upfield chemical shift of resonance 4 is attributed to electric field effects on C_γ of Trp-22 produced by the carboxylate groups of Asp-27 and Asp-9. On the basis of the small difference between the chemical shift of resonance 3 and that of tryptophan C_γ in urea-denatured reductase, it is suggested that W_C may be identified with Trp-6.

Fourier transform nuclear magnetic resonance (NMR), because it allows the direct observation of the behavior of specific atomic nuclei in proteins, has proved a powerful tool for obtaining information about many aspects of the solution behavior of proteins. These include the interaction of specific side chains of the protein with ligands or metal ions, conformational transitions induced in the protein by ligand binding or by changes in temperature or ionic strength, and particularly the dynamics of various motions of the protein (London, 1980). Dihydrofolate reductase (EC 1.5.1.3, DHFR) is especially suitable for such studies because of its rather small size, and reductase from *L. casei* has been investigated by ^{1}H NMR observation of the protein (Feeney et al., 1977; Birdsall et al., 1977; Feeney et al., 1980; Gronenborn et al., 1981a) and by ^{19}F NMR after incorporation of 3-fluorotyrosine and 6-fluorotryptophan (Kimber et al., 1977). However, in these studies relatively little information has been obtained about the dynamics of the motion of this protein until recently (Gronenborn et al., 1981b).

^{13}C NMR has certain advantages in such studies, particularly when the isotope is highly enriched in specific positions of specific side chains. Under such conditions, the very low sensitivity encountered in NMR of natural abundance ^{13}C is largely circumvented, and a relatively simple spectrum is obtained which under ideal conditions shows a single, unsplit resonance for each ^{13}C-enriched side chain in the protein. The

† From the Department of Biochemistry, College of Medicine, The University of Iowa, Iowa City, Iowa 52242 (J.P.G., L.C., and R.L.B.), and the Los Alamos Scientific Laboratory, University of California, Los Alamos, New Mexico 87545 (R.E.L.). *Received April 15, 1981.* This research was performed under the auspices of the U.S. Department of Energy and was supported in part by U.S. Public Health Service Research Grant CA 13840 (R.L.B.) from the National Cancer Institute and Research Grant P41 RR00962-05 from the Division of Research Resources of the National Institutes of Health. Nuclear magnetic resonance spectra at 90.52 MHz were obtained at the Purdue University Biochemical Magnetic Resonance Laboratory which is supported by Biomedical Research Support Grant RR01077 from the National Institutes of Health and at the Colorado State University Regional NMR Center, funded by National Science Foundation Grant CHE 78-18581.
‡ Present address: Abbott Laboratories, North Chicago, IL 60064.

0006-2960/81/0420-6169$01.25/0

great complexity of proton NMR spectra of proteins is thus avoided, and the possible perturbation of the structure of the protein that follows introduction of fluorinated aromatic amino acids for use with ^{19}F NMR (Matthews, 1979) is avoided.

Biosynthetic incorporation of a specifically ^{13}C-enriched amino acid into proteins is most readily accomplished by presenting the labeled amino acid to bacteria growing in a chemically defined medium, and streptococci and lactobacilli are ideal for this purpose since many are auxotrophic for all amino acids. Advantage has been taken of this characteristic to incorporate ^{13}C-labeled methionine (Blakley et al., 1978) and arginine (Cocco et al., 1977, 1978) into DHFR of *Streptococcus faecium* var *Durans*. In the case of bacteria like *Escherichia coli* that are capable of growing on a simple medium, it is sometimes necessary to use a strain auxotrophic for the amino acid to be incorporated. This has been performed by Coleman and his colleagues (Coleman et al., 1978), who used a strain of *E. coli* auxotrophic for histidine to obtain alkaline phosphatase labeled with β,β-dideuterio[γ-^{13}C]-histidine. We now report the incorporation of [γ-^{13}C]tryptophan into DHFR of the strain of *S. faecium* which we have previously used. This is a variant of strain A (Hutchison, 1958; Coultas et al., 1966) which produces almost exclusively one of the two isozymes of DHFR present in the parent organism and in strain A (Nixon & Blakley, 1968).

To obtain the maximum information about both static and dynamic aspects of protein structure from the ^{13}C NMR spectrum of the labeled protein, it is necessary to determine for each resonance the chemical shift, relaxation times (T_1 and T_2), nuclear Overhauser effect (NOE), and also coupling to adjacent nuclei and paramagnetic relaxation when these occur. To obtain this set of parameters, it is necessary that the resonances corresponding to the set of labeled side chains are rather well resolved. Only three of either resonances in the spectrum from [*guanidino*-^{13}C]arginine-labeled DHFR from *S. faecium* are well resolved (Cocco et al., 1977, 1978), and the seven resonances from [*methyl*-^{13}C]methionine-labeled DHFR only approach complete resolution when the enzyme is in a ternary complex with methotrexate (MTX) and NADPH (Blakley et al., 1978). Better resoltuon was obtained for the eight histidine resonances from alkaline phosphatase, especially with certain combinations of metals present (Browne et al., 1976; Coleman et al., 1978).

Complete resolution of the set of resonances depends on the range of chemical shifts and on the number of labeled side chains. As we report here, both of these parameters are favorable in the case of *S. faecium* DHFR labeled with [γ-^{13}C]tryptophan, with the result that NMR spectra suitable for intensive study have been obtained. In particular, the evidence indicates that two of the four tryptophan side chains are in exchange between nonequivalent microenvironments. A preliminary account of these results has been published (London et al., 1979).

Experimental Procedures

Material. L-[γ-^{13}C]Tryptophan (90% ^{13}C) was obtained from KOR Isotopes. L-Amino acids, lysozyme, deoxyribonuclease I, and NADPH were obtained from Sigma. Protamine sulfate was obtained from Krishell Laboratories, Portland, OR, and folic acid from Yodagawa Pharmaceutical Co., Osaka, Japan. Other materials were as previously described (Blakley et al., 1978).

Methods. S. faecium var *Durans* strain A was grown as previously described (Blakley et al., 1978) except as indicated. Purification of DHFR isoenzyme 2 from the bacterial paste was also carried out as described in our previous work (Blakley et al., 1978). Some samples were sufficiently pure (as judged by specific activity) without passage through the affinity column. Enzyme solutions for use in NMR measurements were concentrated by ultrafiltration (Amicon UM10 membrane) and then dialyzed against 0.05 M potassium phosphate buffer, pH* 7.3, containing 0.02% sodium azide, 0.5 M potassium chloride, 1 mM EDTA, and 10–20% D_2O. The last was included to provide a frequency lock for the NMR spectrometer. The reductase concentration in samples was 0.75–1.1 mM. Enzymatic activity was determined as described by Nixon & Blakley (1968), with calculations based on a molar absorbance change of 12 300 (Hillcoat et al., 1967), and is expressed in international units. Activity was unchanged in a week at 5 or 15 °C under conditions used in NMR recording, and in 16 h at 25 °C, the decrease in activity wa less than 20%.

Fourier transform NMR recordings were largely carried out with a Varian XL-100-15 spectrometer at the Los Alamos Scientific Laboratory. The instrument was operated at 25.2 MHz and interfaced with a Nova 1210 computer. Spectra were recorded with a 500-Hz spectral width with 512 data points, a 45-μs (90°) pulse, no pulse delay, and an acquisition time of 1 s. Spectra at 90.5 MHz were obtained on a Nicolet NT-360 spectrometer at the Purdue University Biochemical Magnetic Resonance Laboratory and the Colorado State University Regional NMR Center. The spectrometers are interfaced to Nicolet 1180 computers. Spectra were recorded with a 5000-Hz spectral width, 16 384 data points, a 15-μs (90°) pulse, no pulse delay, and an acquisition time of 1.64 s. Resolution of the 90.52-MHz spectra was enhanced by exponential multiplication of the free induction decay signal leading to 4–10 Hz broadening of the resonances. This broadening was subtracted when peak widths were estimated. All chemical shifts are reported relative to external tetramethylsilane, and unless otherwise noted, spectra were recorded under conditions of proton decoupling. With the Varian XL-100-15, 63 000–144 000 transients were collected for each spectrum; 15 000–24 000 transients were collected with the Nicolet NT-360 for each spectrum. T_1 (spin–lattice relaxation time) and NOE values were determined as previously described (Blakley et al., 1978).

Determination of the effect of frequency on resonance parameters is hampered by associated decoupler-induced sample heating at high fields (Led & Peterson, 1978). For evaluation of this effect, ^1H-coupled ^{13}C spectra were also obtained at 90.5 MHz. The small, long-range couplings were found to contribute negligibly to the line widths, the latter being essentially identical with those measured by using ^1H decoupling. Heating is therefore not a problem.

Calculations of line shape for a ^{13}C nucleus undergoing chemical exchange were carried out with a computer program in Fortran with a Digital Equipment Corp. VAX 11/780 computer. If exchange is assumed between two states A and B, which have fractional populations N_A and N_B, correspond to resonance positions ν_A and ν_B, and have lifetimes τ_A and τ_B, then a line shape can be calculated, provided values of N_A, $(\nu_A - \nu_B)$, τ_A, and the line width in absence of exchange broadening are assumed (Emsley et al., 1965; Drago, 1977). The line width in the absence of exchange was assumed to be 4.0 Hz in the 25.2-MHz spectra and 12 Hz in the 90.5-MHz spectra, the same as the experimental line widths of peaks 1 and 2. For a given value of N_A and of $(\nu_A - \nu_B)$, a series of spectra were generated corresponding to different values of τ_A, and the program estimated and listed the line width for component B for each τ_A. These tables of line widths were

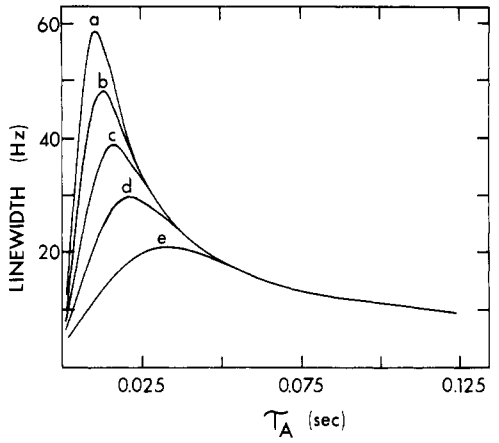

FIGURE 1: Relation between line width at 25.2 MHz and τ_A (residence time in state A) predicted for chemical exchange between two states. The fractional population of state A was set at 0.25, and line widths in the absence of exchange were set at 4 Hz. The separation of the chemical shifts of states A and B ($\nu_A - \nu_B$) were (a) 150, (b) 125, (c) 100, (d) 75, and (e) 50 Hz. For other details, see Experimental Procedures.

Table I: Effect of Tryptophan Concentration in the Growth Medium for *S. faecium* on the Yield of DHFR

Trp concn (mg/L)	final cell density[a]	total DHFR[b] (IU)	DHFR (IU/mg of Trp)
1.9	1.0	117	62
3.8	1.8	163	44
7.5	2.0	166	22

[a] Absorbance at 660 nm when growth ceased and cells were harvested. [b] From cells growing in 1 L of medium.

then scanned for values corresponding to observed line widths under various experimental conditions. Figure 1 shows typical results for the relation of line width to τ_A, with given sets of parameters.

Velocity sedimentation experiments were performed with the use of a double-sector cell in a Model E Spinco ultracentrifuge at a velocity of 60000 rpm. The protein at a concentration of 23 mg/mL was sedimented in 62.5 mM potassium phosphate buffer, pH 7.3, containing 375 mM KCl and 0.02% sodium azide at 20 °C. A single, apparently symmetrical peak was observed corresponding to an uncorrected coefficient of 1.978 S.

Results and Discussion

Biosynthesis of DHFR Containing [γ-^{13}C]Tryptophan. The chemically defined medium previously used (Blakley et al., 1978) was limiting in methionine but contained 0.3 g of tryptophan per L. For the incorporation of labeled tryptophan, the methionine content was increased to 0.141 g/L, and experiments were performed to determine the minimum tryptophan concentration required for good growth and enzyme synthesis. The results, shown in Table I, indicate that although increasing the tryptophan concentration above 2 mg/L approximately doubled the final cell mass present at the point when growth ceased, the total enzyme units recovered from the cells in 1 L of medium only increased by 42%, and the maximum yield of enzyme per milligram of tryptophan was obtained at a concentration of 1.9 mg of Trp/L. This concentration of [γ-^{13}C]tryptophan was therefore used in all incorporation experiments. In a series of preparations performed under these conditions, the yield of cell paste ranged from 1.1 to 2.2 g/L, and the yield of DHFR in the crude cell extract was 40.3–65.6 IU/g of cell paste. The yield of homogeneous DHFR was 1560–7100 IU from a 100-L fermentation, and the specific activity of these preparations varied from 26 to 37 IU/mg of protein.

Table II: Chemical Shifts at 25.2 MHz in ^{13}C NMR Spectra of DHFR Labeled with [γ-^{13}C]Tryptophan (ppm with Respect to External Tetramethylsilane)[a]

conditions (°C)	chemical shifts			
5	111.17	110.50	110.03, 109.82	105.62
15	111.15	110.44	110.00, 109.79	105.75
25	111.11	110.37	109.93, 109.75	106.11
30[b]	111.08	110.34	109.96, 109.74	~106.27
15, in 6 M urea			109.72	

[a] DHFR (0.97 mm) in the presence of 0.05 M potassium phosphate buffer, pH 7.3, 0.5 M KCl, 0.02% sodium azide, 1 mm Na_2EDTA, and 10% (v/v) D_2O. Chemical shifts have been corrected for a lock shift of 0.2 ppm/10 °C. [b] During recording of the spectrum at 30 °C, considerable denaturation and precipitation occurred.

Table III: NMR Parameters at 25.2 MHz for Tryptophan C_γ Resonances from DHFR Labeled with [γ-^{13}C]Tryptophan

temp (°C)	reso-nance	line width (Hz)	T_2 (s)	T_1 (s)	NOE
15	1	4.0	0.080	0.88	1.1
15	2	4.0	0.080	0.87	1.3
15	3	4.0	0.080	1.04	1.3
15	4	18.8	0.170	1.04	1.2
5	4	11.3			
25	4	28.4			

No direct measurements were made of the efficiency of utilization of the [γ-^{13}C]tryptophan in the medium by the bacteria, but since only this amino acid was limiting and since harvesting was performed after growth had ceased, efficient utilization may be assumed. Under analogous conditions, more than 85% of a limiting concentration of [^{14}C]arginine is utilized (Cocco et al., 1978). It is unlikely that label in the incorporated tryptophan was diluted since *S. faecium* does not grow in the absence of an exogenous supply of this amino acid, but this point was not directly demonstrated. However, in the case of the incorporated [^{14}C]arginine, dilution was less than 5%, and the intensity of the resonances from DHFR labeled with [γ-^{13}C]tryptophan is consistent with negligible dilution of isotope.

^{13}C NMR Spectrum for Uncomplexed DHFR. As previously reported (London et al., 1979), in the absence of ligands, the spectrum of DHFR labeled with [γ-^{13}C]tryptophan shows four resonances, one of which (resonance 3) is split into two parts of unequal intensity (Figure 2 and Table II) and another (resonance 4) is very broad with a chemical shift far upfield. The chemical shifts of resonances 1–3 for the uncomplexed enzyme change little with temperature over the accessible range (Table II) whereas the position of resonance 4 moves downfield significantly as the temperature is increased.

Table III shows values of the line width, corresponding spin–spin relaxation time (T_2), spin–lattice relaxation time (T_1), and NOE determined for each of the four resonances at 25 °C, at a carbon resonance frequency of 25.2 MHz. The theoretical basis for the relaxation of a ^{13}C nucleus by dipolar and chemical shift anisotropy (CSA) mechanisms has been examined and experimentally verified by Doddrell et al. (1972) and Norton et al. (1979), respectively. The expressions for $1/T_1^D$, line width^D (dipolar contributions to $1/T_1$ and line width), $1/T^{CSA}$, line width^{CSA} (contributions to $1/T_1$ and line

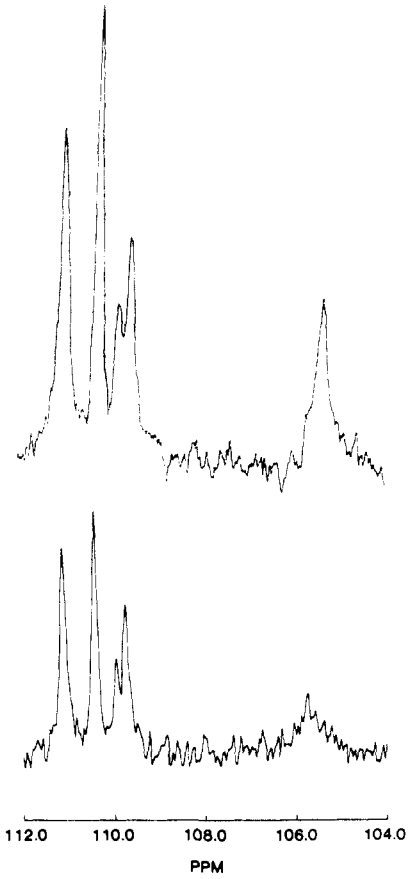

FIGURE 2: ^{13}C NMR spectra of *S. faecium* DHFR labeled with [γ-^{13}C]tryptophan. The lower spectrum (144 324 transients) was obtained at 25.2 MHz and the upper (18 000 transients) at 90.5 MHz. Both spectra were obtained at 5 °C. For other details, see Experimental Procedures.

width from the CSA relaxation mechanism), and NOE for the isotropic rigid rotor model are

$$\frac{1}{T_1^D} = \frac{1}{10}\left(\frac{\gamma_H^2\gamma_C^2\hbar^2}{r_{CH}^6}\right)\chi_H$$

$$\text{line width}^D = \frac{1}{20}\left(\frac{\gamma_H^2\gamma_C^2\hbar^2}{r_{CH}^6}\right)\phi_H$$

$$\text{NOE} = 1 + \frac{\gamma_H}{\gamma_C(\chi_H + \omega'_{1C})}\left(\frac{6\tau_R}{1 + (\omega_H + \omega_C)^2\tau_R^2} - \frac{\tau_R}{1 + (\omega_H - \omega_C)^2\tau_R^2}\right)$$

$$\chi_H = \frac{\tau_R}{1 + (\omega_H - \omega_C)^2\tau_R^2} + \frac{3\tau_R}{1 + \omega_C^2\tau_R^2} + \frac{6\tau_C}{1 + (\omega_H + \omega_C)^2\tau_R^2}$$

$$\phi_H = \chi_H + 4\tau_R + \frac{6\tau_R}{1 + \omega_H^2\tau_R^2}$$

$$\frac{1}{T_1^{CSA}} = (2/15)\gamma^2H_0^2(\Delta\sigma)^2\tau_R(1 + \gamma^2H_0^2\tau_R^2)^{-1}$$

$$\text{line width}^{CSA} = (45\pi)^{-1}\gamma^2H_0^2(\Delta\sigma)^2\tau_R[4 + 3(1 + \gamma^2H_0^2\tau_R^2)^{-1}]$$

where γ = gyromagnetic ratio, H_0 = magnetic field strength,

Table IV: Literature Values for Chemical Shifts of C_γ of Tryptophan and of Tryptophanyl Residues in Peptides

compound	pH	δ	reference
Trp	1.1	107.23	London (1981)
Trp	6.7	108.50	London (1981)
Trp	11.8	111.95	London (1981)
Trp	4.0	108.54	Allerhand et al. (1973)
Trp	2.0	107.2	Bradbury & Norton (1973)
Gly-Trp	~2	109.9	Bradbury & Norton (1973)
Gly-Trp-Gly	~2	109.9	Bradbury & Norton (1973)
Trp-Trp	~2	106.9, 109.5	Bradbury & Norton (1973)
Trp-Ser-Tyr-Gly	3.1	107.2	Wessels et al. (1973)
⟨Glu-His-TrpNH$_2$	7.6	109.93	Deslauriers et al. (1975)
⟨Glu-His-Trp-Ser-Tyr-Gly	2.55	109.8	Wessels et al. (1973)
LH-RH[a]	5.45	109.6	Wessels et al. (1973)
LH-RH[a]	6.4	109.65	Deslauriers et al. (1975)
des-Gly^{10}-LH-RH[a]	6.4	110.07	Deslauriers et al. (1975)
des-Gly^{10}-LH-RH[a]	6.3	109.61	Deslauriers et al. (1975)

[a] LH-RH, luteinizing hormone-releasing hormone. This has the structure ⟨Glu-His-Trp-Ser-Tyr-Gly-Leu-Arg-Pro-GlyNH$_2$, where ⟨Glu indicates a pyroglutamate residue.

$\Delta\sigma$ = 200 ppm [see Norton et al. (1977)], τ_R = rotational correlation time, ω = resonance frequency in radian per second, r_{CH} = distance between the ^{13}C and ^1H nuclei, and ω'_{1C} = other spin–lattice relaxation contributions including CSA.

If it is assumed that the dipolar interaction is dominated by the intraresidue ^{13}C–^1H interaction (Oldfield & Allerhand, 1975b) and the estimate of $\Delta\sigma$ = 200 ppm suggested by Norton et al. (1977) is used with our previously determined rotational correlation time of 2×10^{-8} s for overall molecular tumbling (Cocco et al., 1978), the calculation gives the following relaxation parameters: T_1^D = 1.5 s, T_1^{CSA} = 4.1 s, T_2^D = 0.2 s, T_2^{CSA} = 0.56 s, and NOE = 1.15. The net spin–lattice relaxation time of 1.09 s is in reasonably close agreement with the measured values in Table III. This result tends to rule out the possibility of rapid (compared with the rate of overall molecular tumbling) large-amplitude internal motion of the Trp side chain. The small discrepancies could reflect interresidue dipolar contributions, approximations inherent in the CSA calculation given by Norton et al. (1977) (Lynden-Bell, 1975; Spiess, 1979), low amplitude internal motion, or a variety of other factors. The calculated line width based on the spin–spin relaxation rate indicates that nearly half the observed line width of resonances 1–3 reflects field inhomogeneity or exchange broadening.

Measurement at a ^{13}C frequency of 90.5 MHz confirms the greater importance of the CSA relaxation mechanism at this field. Calculated relaxation parameters assuming the same τ and $\Delta\sigma$ values as above are T_1^D = 16.1 s, T_1^{CSA} = 4.0 s, line width^{CSA} = 7.3 Hz, and NOE = 1.15. With the assumption that the measured line width for resonances 1 and 2 at 25.2 MHz contains a negligible CSA contribution, the calculated line width at 90.5 MHz of 4.0 + 7.3 = 11.3 Hz is in good agreement with the measured value of 12 Hz for resonances 1 and 2. The observed high field T_1 was determined approximately as 2.9 s, also in reasonable agreement with the net predicted value of 3.2 s.

Since the NOE for all four resonances is very similar and since the peak area is similar in all cases as judged by computer integration and by the cut and weigh procedure, it is clear that each peak must correspond to the resonance from one of the four ^{13}C-labeled tryptophans shown to be present in *S. faecium* DHFR (Gleisner et al., 1974). The labeled tryptophan side chains corresponding to resonances 1–4 will be arbitrarily designated W_A, W_B, W_C, and W_D, respectively.

In Table IV the chemical shifts of these four resonances are compared with that of Trp C_γ in urea-denatured DHFR (Table II), in free Trp at various pH values, and in small peptides. The major resonance from random coil DHFR has a δ very similar to that for C-terminal Trp at low pH and for internal Trp. It is also similar to that for one of two resonances (109.9, 111.0) reported for α-chymotrypsin in 6 M guanidine hydrochloride at pH 2.7 (Bradbury & Norton, 1973).

Resonances 1–3 have chemical shifts within 1.43 ppm of that for random coil DHFR, but resonance 4 is 4.0 ppm upfield from the latter and 3 ppm upfield from the Trp C_γ shifts observed in hen egg white lysozyme, cytochrome *c*, hemoglobin, and myoglobin (Oldfield & Allerhand, 1975a,b; Oldfield et al., 1975), and several peptides (Bradbury & Norton, 1973). An upfield shift of this magnitude cannot be attributed solely or even principally to ring current effects of adjacent aromatic rings. When the closest approach of another aromatic ring is used with appropriate contour diagrams (Perkins & Dwek, 1980), it can be calculated that stacking of an aromatic ring on either side of the ^{13}C-labeled tryptophan residue produces a maximum shift change from the random coil value of about 2 ppm. This prediction is consistent with differences between δ for tryptophan protons in lysozyme and the random coil value (Perkins & Dwek, 1980). Other sources of shift changes of ^{13}C resonances are conformationally dependent phenomena, such as the γ effect (Woolfenden & Grant, 1966; Grant & Cheney, 1967). However, such effects are improbable for Trp C_γ since steric compression of the type involved in these effects cannot occur.

The most likely source of this large upfield shift is electric field effects to which Trp C_γ is very sensitive. Thus δ for C_γ in free Trp changes by 4.72 ppm as the amino acid changes its ionization state (Table IV). This is 3-fold greater than the corresponding effects at other ring carbons (London, 1981) or for C_γ of leucine (Tran-Dinh et al., 1974). Major changes in chemical shift at carbons involved in unsaturated bonds have been predicted by the calculations of Batchelor (1975), Seidman & Maciel (1977), and specifically for amino acids by Horsley & Sternlicht (1968).

Evidence for Chemical Exchange for W_C and W_D. As previously pointed out (London et al., 1979), the characteristics of resonances 3 and 4 indicate that W_C and W_D are each involved in chemical exchange processes. The double structure of resonance 3 is unlikely to be due to scalar coupling of the spin of C_γ to that of another nucleus with $S = 0.5$. Since all the protons were decoupled under the conditions of recording used, scalar ^1H–^{13}C coupling cannot be responsible. The low natural abundance of ^{13}C (1.108%) at nonenriched positions, together with the low probability of through-space ^{13}C–^{13}C coupling, also eliminates ^{13}C–^{13}C scalar coupling. Furthermore, scalar coupling is excluded as the cause by the frequency dependence of the splitting of resonance 3. The splitting at 25.2 and 90.5 MHz is the same [0.20 and 0.21 ppm, respectively (Figure 1)], but the chemical shift difference in hertz is field dependent (5 and 19 Hz, respectively).

Slow reversible aggregation of the protein with resulting perturbation of the magnetic field at W_C, but not at the other tryptophans, was also eliminated as an explanation. There was no aggregation during velocity sedimentation at concentrations from 3.3 mg/mL (Nixon & Blakley, 1968) to the highest concentrations used in the NMR experiments (see Experimental Procedures). In sedimentation at the highest concentration range, conditions were very similar to those used in the NMR studies. Another possible explanation of the splitting of resonance 3 on the basis of a slow equilibrium between protonated and unprotonated states of a histidine near W_C was eliminated by the demonstration that the splitting is unchanged over the pH range 6.55–9.83.

From simulation of the line shape of resonance 3 obtained at 15 °C (Figure 2), it could be determined that the populations of W_C in the two states corresponding to peaks 3A and 3B are in the ratio 2:3. No change in the ratio of these populations could be detected at 5 or 25 °C, and the peak separation ($\nu_A - \nu_B$) was also unchanged. Since this behavior is consistent with slow exchange, the limit $\tau_A \gg (\nu_A - \nu_B)^{-1}$ can be placed on the lifetime in state A. This leads to lower limit of 0.03 s for the lifetime in state A and 0.045 s in state B. Line-shape simulation suggested that the lower limit of τ_A and τ_B is 0.5 and 0.75 s, respectively. We have subsequently observed that the 3A/3B ratio is dependent on additional factors, including the salt concentration in the buffer (R. E. London, J. P. Groff, and R. L. Blakley, unpublished results).

Resonance 4 has considerably greater line width at 15 °C than the other resonances: about 18.8 Hz at half-height compared with 4 Hz for resonances 1 and 2. The line width of resonance 4 also shows temperature dependence (Table III), and this again distinguishes it from the other three resonances which do not change in line width with temperature (London et al., 1979). Moreover, there is a considerable downfield change in chemical shift for resonance 4 (0.6 ppm) as the temperature is increased from 5 to 30 °C whereas there is little temperature dependence of the chemical shift of the other resonances (Table II). This behavior is clearly related to chemical exchange of W_D, but two different interpretations are possible.

The effects of temperature on line width and chemical shift were previously interpreted as indicating that W_D is in slow exchange and that the exchange rate increases with temperature, but N_A and ($\nu_A - \nu_B$) are unchanged (London et al., 1979). On this interpretation, the observed resonance 4 is resonance 4B, and another component, resonance 4A, must be assumed present in the spectrum but unobserved because its population is low and its line width is great and perhaps because its chemical shift is in the same region as resonances 1, 2, or 3. However, when parameters in a two-state, slow-exchange model (see Experimental Procedures) were selected for best fit to the observed line shapes at 25.2 MHz, these parameters predicted line widths at 90.5 MHz much lower than the observed values.

An alternative interpretation is that W_D is in intermediate to fast exchange, with N_A increasing with temperature. If this interpretation is correct, values of N_A and ($\nu_A - \nu_B$) can be found, which at appropriate values of τ_A correctly predict the line widths observed at both 25.2 and 90.5 MHz at 5, 15, and 25 °C, respectively. These parameters should also correctly predict the change in chemical shift for resonance 4 with temperature. Table V shows that the line shapes observed at 25.2 MHz at various temperatures can be closely matched by choosing appropriate parameters. The solutions were reached by starting with minimum values of N_A for which a τ_A value could be found in the fast region that gives the desired line widths at 25.2 MHz. It may be seen that the parameters

Table V: Observed Line Widths and Chemical Shifts for Resonance 4 at Different Temperatures and Best-Fit Line Widths with Corresponding Parameters

obsd					corresponding exchange parameters[b]			
temp (°C)	line width (Hz)	δ (ppm)	Δδ (ppm)	best-fit line width[a] (Hz)	Δδ (ppm)	N_A	τ_A (ms)	ν_e[c] (s^{-1})
5	11.3	105.62		11.25		0.062	1.84	92
15	18.8	105.72	0.10	18.75	0.20	0.13	1.52	120
25	28.4	106.11	0.49	28.25	0.67	0.24	1.36	154

[a] Best-fit line widths were calculated on the assumption that the value of $(\nu_A - \nu_B)$ was 100 Hz. [b] Values corresponding to the best-fit line width. [c] ν_e, the exchange rate, $= 1/2\pi\tau$.

Table VI: Comparison of Observed and Predicted Line Widths and Chemical Shifts at 90.5 MHz

obsd				predicted[a]	
temp (°C)	line width	δ	Δδ	line width	Δδ
5	26.0	105.49		25	
15	52.0	105.52	0.03	48	0.05
25	120	105.56	0.07	116	0.16

[a] Calculated by the use of a $(\nu_A - \nu_B)$ value of 360 Hz and the exchange parameters to give the best fit to corresponding line widths at 25.2 MHz (see Table V).

giving best-fit line shapes also predicted changes in chemical shift that approximate reasonably well to the observed values, especially when it is considered that experimental chemical shifts are accurate only to ±0.04 ppm. The parameters that gave best-fit line widths at 25.2 MHz were used to calculate line widths and chemical shifts at 90.5 MHz, and these predictions are compared to observed values in Table VI. The agreement is clearly satisfactory.

The solutions given in Table V are probably not unique, but appropriate line shapes cannot be generated if large changes are made in the parameter values. Thus a change of $(\nu_A - \nu_B)$ to 75 or 125 Hz with τ_A values that give a line width of 28.4 Hz at 25.2 MHz led to too large line widths at 90.5 MHz. If $(\nu_A - \nu_B)$ was kept at 100 Hz but N_A values were all increased, the values of ν_e no longer increased with temperature. It seems likely therefore that the allowed values of $(\nu_A - \nu_B)$ and N_A are close to those in Table V. It will be noted that the values of ν_e are of the same order as those of $(\nu_A - \nu_B)$ or greater and significantly greater than that calculated from resonance 3 for W_C. The fit of the line shapes calculated from the parameters in Table V to resonance 4 in the experimental spectra are shown in Figure 3. Finally, we note that the motion associated with ν_e is considerably slower than overall molecular tumbling and thus is not expected to significantly alter T_1, as observed.

From the values of N_A in Table V, corresponding $\Delta G°$ values can be calculated for conversion of the enzyme in state B to state A. Values are +1.50, +1.09, and +0.68 kcal mol^{-1} at 5, 15, and 25 °C, respectively. A van't Hoff plot of ln K vs. $1/T$ gave a mean value for ΔH of +13 kcal mol^{-1} over this temperature range. This in turn yields a mean entropy change of +41 cal deg^{-1} mol^{-1}. However, it is likely that ΔH in fact changes with temperature (cf. Sturtevant, 1977).

It should be noted that although the above treatment of the exchange process for W_D is in terms of a two-state model, there is nothing in the data which precludes the existence of an equilibrium between a continuum of many states for W_D. The data are then interpreted as indicating a shift of the equilibrium with increasing temperature toward the states with higher free energy, which are also associated with a chemical shift for W_D closer to that for urea-denatured enzyme. Since, as

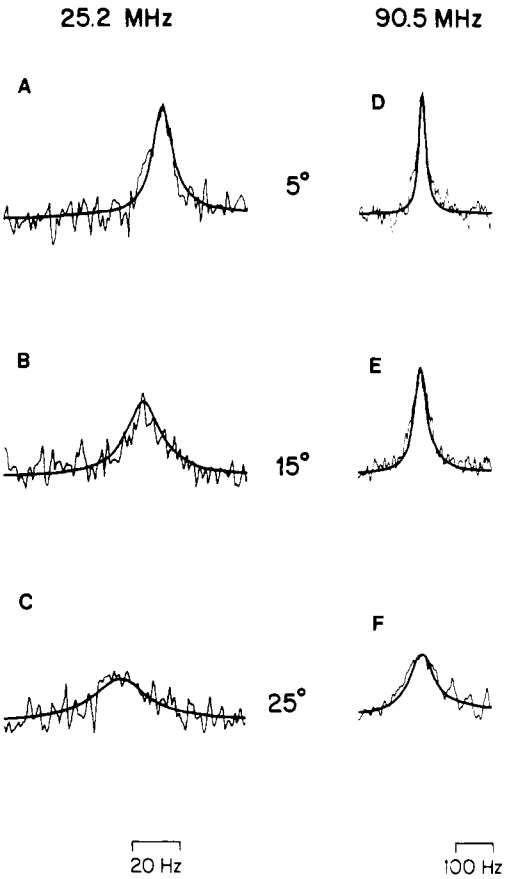

FIGURE 3: Fit of line shapes generated by using parameters in Table VI to resonance 4 in the experimental spectra. Curves A, B, and C were taken from the region between 104 and 108 ppm from spectra obtained at 25.2 MHz, and spectra D, E, and F were taken from the region between 103 and 107 ppm from spectra obtained at 90.5 MHz. Curves a and d were obtained at 5 °C, b and e at 15 °C, and c and f at 25 °C. Spectra a (144 324 transients), b (63 309 transients), and c (116 470 transients) and e (23 400 transients) were processed with no line broadening, spectra d (18 000 transients) and e (23 400 transients) with 4-Hz line broadening, and spectrum f (15 000 transients) with 10-Hz line broadening. For other details, see the text.

discussed below, the exchange process probably represents equilibrium between different conformational states of the protein, the contribution of many states is very likely.

Molecular Basis of the Chemical Exchange Involving W_C and W_D. The evidence presented in the preceding section establishes that W_C and W_D, the tryptophan residues corresponding to resonances 3 and 4, are undergoing exchange between different microenvironments. Alternative explanations of these exchange processes in molecular terms are as follows. (1) The tryptophan side chains may undergo complete or partial rotation about the C_α–C_β and C_β–C_γ bonds in motion analogous to that observed for tyrosine and phenylalanine rings (Campbell et al., 1976; Wüthrich & Wagner, 1975; Hull &

Scheme I: Carboxy-Terminal Sequences of DHFR from *L. casei* and *S. faecium* II[a]

alignment A

L. casei Thr-Asn-Pro-Ala-Leu-Thr-His-Thr-Tyr-Glu-Val-Trp-Gln-Lys-Lys-Ala

S. faecium Gln-Tyr-Pro-His-Arg-Phe-Gln-Lys-Trp-Gln-Lys-Met-Ser-Lys-Val-Val

alignment B

L. casei Thr-Asn-Pro-Ala-Leu-Thr-His-Thr-Tyr-Glu-Val-Trp-Gln-Lys-Lys-Ala

S. faecium Asn-Gln-Tyr-Pro-His-Arg-Phe-Gln-Lys-Trp-Gln-Lys-Met-Ser-Lys-Val-Val

[a] Underlined residues constitute strand βH of the β sheet.

Sykes, 1975). (2) The tryptophan residues might be moving with a flexible segment of backbone which is not constrained by involvement in the secondary structure of the protein. In this case, the tryptophan residue happens to monitor motion that is shared to a greater or lesser degree by a number of adjacent residues. (3) The exchange might reflect primarily the internal motion, not of the tryptophan residue but of another residue (residues) which produces (produce) major effects on the magnetic field experienced by the tryptophan C_γ. In the case of W_D this would correspond to internal motion of the charged side chain that produces the electric field responsible for the large upfield shift of resonance 4.

The large size and asymmetry of the tryptophan nucleus compared with phenylalanine and tyrosine make the first explanation rather unlikely, especially when it is considered that tryptophans are usually found in rather tightly packed, hydrophobic environments. This is the case, for example, in the *L. casei* DHFR structure. At most, a minor contribution is probably to be expected from such motion. The second or third type of motion, or a combination of them, seems a more plausible basis for the exchange process. This is discussed further in connection with tentative assignments of the resonances.

Structural Assignment of Tryptophan Resonances. *S. faecium* DHFR has not been subjected to X-ray crystallography, so that it is not yet possible to use a crystallographic model of the protein to determine what neighboring side chains perturb the shielding at C_γ of each of the four tryptophan residues in the known sequence of the enzyme. On the other hand, a crystallographic model of the ternary complex of *L. casei* DHFR with methotrexate and NADPH is available, and this provides an approximation to the structure of the *S. faecium* enzyme, provided it is assumed that (1) the backbone conformation of the *L. casei* and *S. faecium* enzymes is similar, (2) the two sequences can be properly aligned, and (3) corresponding side chains in the two structures are similarly oriented.

No direct evidence for the first of these assumptions can yet be provided, and such an assumption must be treated with great caution. However, the backbone conformations of *E. coli* and *L. casei* DHFR can be compared because both enzymes have been examined by X-ray crystallographic diffraction. When 142 out of the 159 α-carbon coordinates in the methotrexate binary complex of *E. coli* DHFR (Matthews et al., 1977) are matched by least squares to structurally equivalent α-carbon coordinates for the methotrexate–NADPH ternary complex of *L. casei* DHFR (Matthews et al., 1978), the root mean square deviation is 1.7 Å (Matthews et al., 1979). Thus, despite rather low sequence homology between DHFR from these two sources, the geometry of the peptide backbone is nevertheless almost identical in the two structures, the only significant differences being found in loops connecting elements of secondary structure. Solution of the structure of the chicken liver enzyme has shown that it also has a backbone conformation closely resembling that of the bacterial enzymes, except for three major insertions (D. A. Matthews, personal communication). Since DHFRs from *S. faecium* (isozyme 2) and *L. casei* show about the same degree of sequence homology as the *L. casei* and *E. coli* enzymes, it is not unreasonable to suppose that there is also a close similarity in the three-dimensional arrangement of the peptide backbone for the *L. casei* and *S. faecium* 2 structures. If this is case, then when structurally equivalent backbone atoms of these two DHFR's are appropriately aligned, the β carbons of each amino acid residue involved in the secondary structure (α helices and β sheets) must also be aligned, so that the directions of side chains of such residues in one structure can be predicted from the other.

The question of the appropriate alignment of the sequences of DHFR from vrious sources has been addressed elsewhere (Blakley, 1981). According to this analysis, tryptophans 6, 22, 115, and 160 of the *S. faecium* 2 sequence correspond to Trp-5, Trp-21, Leu-114, and Tyr-155 of the *L. casei* sequence. The alignment of the C-terminal portion of the sequences is the least certain, and another possibility for this region is shown in Scheme I. According to this alternative, Trp-160 of *S. faecium* 2 reductase corresponds to Trp-158 of *L. casei* DHFR (alignment B) instead of to Tyr-155 (alignment A). Although alignment B has more identical residues and conservative changes in corresponding positions of the sequences, it has a number of problems. It leaves a tail of three amino acid residues at the carboxyl end, and it aligns Pro-154 of the *S. faecium* sequence with a region of the *L. casei* sequence involved in β sheet. The latter is unlikely since proline is rarely found in β-sheet structure. For alignment A, the extra residues of the *S. faecium* sequence are accommodated in the loop connecting βH to βG, and Pro-154 is in this loop rather than in a stretch of β sheet. Alignment A may also allow the aromatic side chain of Trp-160 to be stacked with the aromatic side chains of Phe-30 and Trp-115. In *E.* Coli DHFR, Trp-30 and Phe-153 correspond to Phe-30 and Trp-160 in the *S. faecium* sequence, and X-ray crystallography of the *E. coli* enzyme shows that the rings of Trp-30 and Phe-153 are stacked. Finally, the recently solved structure of the chicken liver reductase also suggests that alignment A is the correct one (D. A. Matthews, personal communication).

From these sequence alignments and on the assumption that *L. casei* DHFR provides a reasonably close structural analogue of *S. faecium* DHFR, some tentative proposals can be made about assignments of the four resonances in the NMR spectra to specific tryptophan residues. It has been pointed out above that the fast exchange involving W_D probably represents movement of a segment of backbone that includes this residue or movement of a charged residue in the vicinity of the tryptophan, or both. With the sequence alignments proposed above, tryptophans 6, 115, and 160 of *S. faecium* DHFR correspond to Trp-5, Leu-114, and Tyr-155 in the *L. casei* structure. These residues are attached respectively to strands

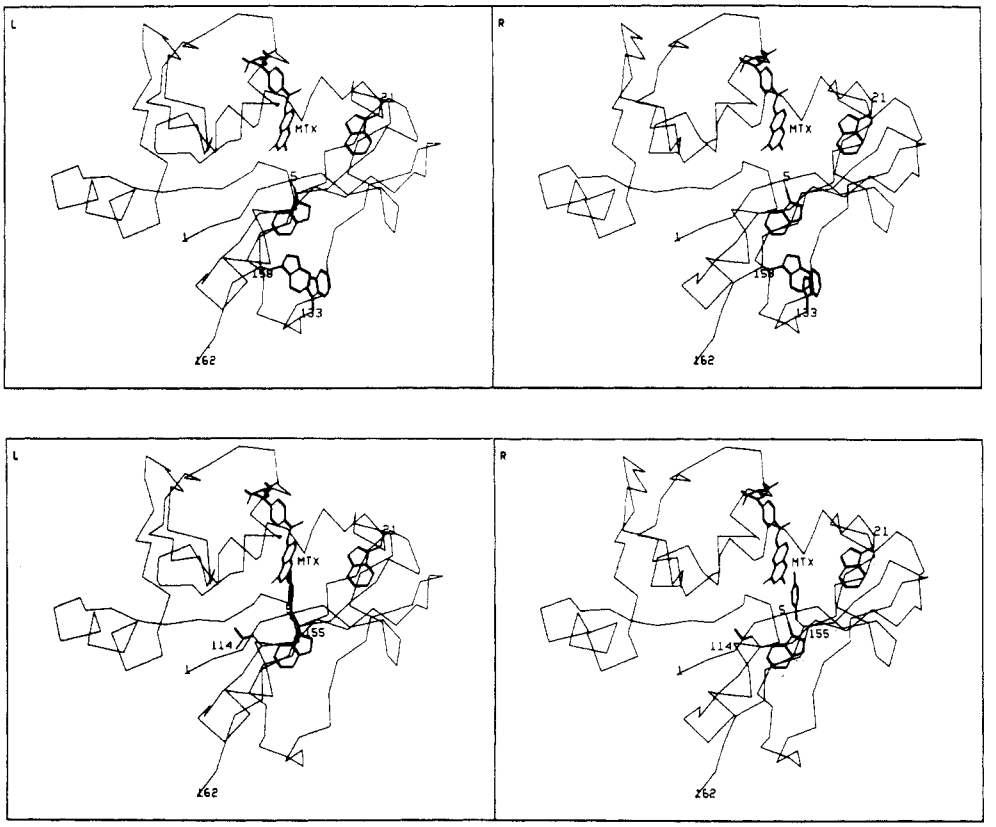

FIGURE 4: Stereo diagrams of the *L. casei* DHFR backbone and certain side chains computed from X-ray crystallographic coordinates for the MTX–NADPH ternary complex. (Upper diagram) Backbone and tryptophan residues in *L. casei*. (Lower diagram) Backbone and side chains of *L. casei* that correspond to tryptophans in the *S. faecium* isozyme 2 sequence. In these diagrams, the backbone is represented by connections between α-carbon atoms, and NADPH has been omitted for further simplification. The pteridine ring of methotrexate is in the active side cavity, the right side of which includes Trp-21. The βA strand, to which Trp-5 is attached, forms part of the bottom of the cavity. The glutamate moiety of MTX may be clearly seen draped over the αB helix.

βA, βF, and βH of β sheet (Figure 4). Only Trp-22, corresponding to Trp-21 in the *L. casei* structure, is attached to a region of backbone not involved in secondary structure. It is in a loop connecting βA to αB (Figure 4) and is one of two loops represented by relatively weak density in the 2.5-Å map for the binary complex of methotrexate with *E. coli* DHFR (Matthews et al., 1979). This suggests that the loop is rather flexible in the binary complex. In contrast, the main-chain and side-chain electron density for this loop is well-defined in the *L. casei* ternary complex (with methotrexate and NADPH), an observation which suggests the binding of NADPH restricts the movement of the loop. Although no X-ray data are available for the uncomplexed enzyme, it is not unlikely that in the absence of ligands this loop is involved in still greater motion which would be adequate to account for the rapid exchange involving W_D. It is therefore reasonable to assume that W_D is Trp-22. The marked sharpening of resonance 4 in the complex with 3′,5′-dichloromethotrexate (London et al., 1979) is consistent with this assignment since interactions of the ligand with residues in this loop would be expected to decrease its mobility.

If the identification of W_D with Trp-22 is correct, then it should be possible to specify which charged amino acid residues are responsible for the unusual upfield chemical shift of resonance 4. By analogy with the *L. casei* DHFR structure, Trp-22 is presumably one of the residues forming one side of the catalytic site cavity of the *S. faecium* enzyme. This cavity is lined with nonpolar residues, the only charged residue being Asp-27 (Asp-26 in the *L. casei* sequence). In the *L. casei* crystal structure, the charged carboxyl group is 7.8 Å from C_γ of Trp-21, so it is reasonable to assume a distance of this order between the carboxyl of Asp-27 and C_γ of Trp-22 in the *S. faecium* enzyme. In the *S. faecium* sequence, there is also an aspartate residue at position 9 which corresponds to Asn-8 in the *L. casei* sequence. In the *L. casei* crystal structure, the carboxamide group of Asn-8 is 7.8 Å from C_γ of Trp-21, so a distance of similar magnitude presumably separates the carboxyl of Asp-9 from C_γ of Trp-22 in the *S. faecium* structure. If it is assumed that these distance estimates are valid and if the electric field effects calculated for charged groups at similar distances from ethylenic and acetylenic bonds (Seidman & Maciel, 1977; Batchelor, 1975) are a reasonable guide, it appears that the charge on one or both of the aspartate carboxyls may be responsible for the upfield shift of resonance 4. Much additional information is required in order to perform a more quantitative treatment. The next nearest charged group to C_γ of Trp-22 is probably Arg-23, but this is on the other side of the backbone from Trp-22; the best estimate of the distance of the positive charge from C_γ of Trp-22 is $\sim$8 Å.

While the evidence thus points to Trp-22 as the residue responsible for resonance 4, the identification of W_C is much more difficult. Exchange for this residue is considerably slower, and this is consistent with the fact that all the other tryptophan side chains are in regions of β sheet where the backbone would have little flexibility. Moreover, the side chains of these tryptophans are probably in closely packed, hydrophobic regions where their movement is strongly hindered by other nonpolar side chains. Since resonance 3 has a chemical shift close to that of tryptophan C_γ in the denatured protein, W_C must be unperturbed by ring current effects or electric field effects. Table VII summarizes the probable environments of the four tryptophan residues as determined from inspection of the *L. casei* model with appropriate re-

Table VII: Environment of Tryptophan Residues in *S. faecium* DHFR

residue	environment	perturbing residues
6	buried in hydrophobic region below substrate pocket	Phe-104, Phe-128, Phe-134
22	partly buried in hydrophobic lining of pocket	Asp-9, Asp-27, Phe-123
115	partly buried in hydrophobic pocket	Phe-30, His-34, Lys-38
160	partly buried in hydrophobic pocket, at end of active site	Phe-30, His-143, Asp-27

placements of side chains from comparison of the appropriately aligned *L. casei* and *S. faecium* sequences. Although these predictions are tentative, they provide at least a first approximation of the microenvironments of each tryptophan side chain. It may be seen from Table VII that positively and negatively charged groups are probably in the vicinity of both Trp-115 and Trp-160 and may in fact be quite close. The magnitude of the electric field effect that will be produced at C_γ of these tryptophan residues is impossible to predict since it will depend on many factors, including the distance of the charge from the C_γ nucleus. In particular, movement of shielding electrons depends on the angle made by the vector joining the charge to the midpoint of the bond and the axis of the bond. Detailed structural information is necessary to determine the latter. However, because of the much larger changes in chemical shift caused by electric field effects as compared with ring current effects, it would not be unreasonable to propose that Trp-6 should be tentatively identified with W_C, the residue corresponding to peak 3 (0.18 ppm downfield from denatured protein), and Trp-115 and Trp-160 identified with W_A and W_B (1.43- and 0.72-ppm downfield from denatured protein, respectively).

Clearly these assignments must be checked by other methods, including the effects of ligand binding, spin-labeled ligands, and modification of specific tryptophan residues. Such studies are in progress and will be reported later.

Acknowledgments

We thank Dr. Jack S. Cohen for obtaining some preliminary spectra at high field (67.9 MHz). We are particularly indebted to Dr. David A. Matthews for generously making available the atomic coordinates of the *L. casei* dihydrofolate reductase ternary complex with methotrexate and NADPH and for valuable comments and advice. We also gratefully acknowledge the assistance of Patrick Briley in producing the stereo diagrams.

References

Allerhand, A., Childers, R. F., & Oldfield, E. (1973) *Biochemistry 12*, 1335–1341.

Batchelor, J. G. (1975) *J. Am. Chem. Soc. 97*, 3410–3415.

Birdsall, B., Griffiths, D. V., Roberts, G. C. K., Feeney, J., & Burger, A. (1977) *Proc. R. Soc. London, Ser. B. 196*, 251–265.

Blakley, R. L. (1981) in *Molecular Actions and Targets for Cancer Chemotherapeutic Agents*, (Sartorelli, A., Ed.) Vol. 2, pp 303–332, Academic Press, New York.

Blakley, R. L., Cocco, L., London, R. E., Walker, T. E., & Matwiyoff, N. A. (1978) *Biochemistry 17*, 2284–2293.

Bradbury, J. H., & Norton, R. S. (1973) *Biochim. Biophys. Acta 328*, 10–19.

Browne, D. T., Earl, E. M., & Otvos, J. D. (1976) *Biochem. Biophys. Res. Commun. 72*, 398–403.

Campbell, I. D., Dobson, C. M., Moore, G. R., Perkins, S. J., & Williams, R. J. P. (1976) *FEBS Lett. 70*, 96–100.

Cocco, L., Blakley, R. L., Walker, T. E., London, R. E., & Matwiyoff, N. A. (1977) *Biochem. Biophys. Res. Commun. 76*, 183–188.

Cocco, L., Blakley, R. L., Walker, T. E., London, R. E., & Matwiyoff, N. A. (1978) *Biochemistry 17*, 4285–4290.

Coleman, J. E., Chlebowski, J. F., Otvos, J. D., Shoot Uiterkamp, A. J. M., & Armitage, I. M. (1978) *Trans. Am. Crystallogr. Assoc. 14*, 17–37.

Coultas, M. K., Albrecht, A. M., & Hutchison, D. J. (1966) *J. Bacteriol. 92*, 516–517.

Deslauriers, R., Levy, G. C., McGregor, W. H. Sarantakis, D., & Smith, I. C. P. (1975) *Biochemistry 14*, 4335–4343.

Doddrell, D., Glushko, V., & Allerhand, A. (1972) *J. Chem. Phys. 56*, 3683–3689.

Drago, R. S. (1977) *Physical Methods in Chemistry*, p 257, W. B. Saunders, Philadelphia, PA.

Emsley, J. W., Feeney, J., & Sutcliffe, L. H. (1965) *High Resolution Nuclear Magnetic Resonance Spectroscopy*, Vol. 1, pp 484–488, Pergamon Press, New York.

Feeney, J., Roberts, G. C. K., Birdsall, B., Griffiths, D. V., King, R. W., Scudder, P., & Burgen, A. (1977) *Proc. R. Soc. London, Ser. B. 196*, 267–290.

Feeney, J., Roberts, G. C. K., Thomson, J. W., King, R. W., Griffiths, D. V., & Burgen, A. S. V. (1980) *Biochemistry 19*, 2316–2321.

Gleisner, J. M., Peterson, D. L., & Blakley, R. L. (1974) *Proc. Natl. Acad. Sci. U.S.A. 71*, 3001–3005.

Grant, D. M., & Cheney, B. V. (1967) *J. Am. Chem. Soc. 89*, 5315–5318.

Gronenborn, A., Birdsall, B., Hyde, E. I., Roberts, G. C. K., Feeney, J., & Burgen, A. S. V. (1981a) *Biochemistry 20*, 1717–1722.

Gronenborn, A., Birdsall, B., Hyde, E. I., Roberts, G. C. K. Feeney, J., & Burgen, A. S. V. (1981b) *Nature (London) 290*, 273–274.

Hillcoat, B. L., Nixon, P. E., & Blakley, R. L. (1967) *Anal. Biochem. 21*, 178–189.

Horsley, W. J., & Sternlicht, H. (1968) *J. Am. Chem. Soc. 90*, 3738–3748.

Hull, W. E., & Sykes, B. D. (1975) *J. Mol. Biol. 98*, 121–153.

Hutchison, D. J. (1958) *Cancer Res. 18*, 214–219.

Kimber, B. J., Griffiths, D. V., Birdsall, B., King, R. W., Scudder, P., Feeney, J., Roberts, G. C. K., & Burgen, A. S. V. (1977) *Biochemistry 16*, 3492–3500.

Led, J. J., & Peterson, S. B. (1978) *J. Magn. Reson. 32*, 1–17.

London, R. E. (1980) in *Magnetic Resonance in Biology* (Cohen, J. S., Ed.) Vol. 1, pp 1–69, Wiley, New York.

London, R. E. (1981) *Org. Magn. Reson.* (in press).

London, R. E., Groff, J. P., & Blakley, R. L. (1979) *Biochem. Biophys. Res. Commun. 86*, 779–786.

Lynden-Bell, R. M. (1975) *Mol. Phys. 29*, 301–302.

Matthews, D. A. (1979) *Biochemistry 18*, 1602–1610.

Matthews, D. A., Alden, R. A., Bolin, J. T., Ereer, S. T., Hamlin, R., Xuong, N., Kraut, J., Poe, M., Williams, M., & Hoogsteen, K. (1977) *Science (Washington, D.C.) 197*, 452–455.

Matthews, D. A., Alden, R. A., Bolin, J. T., Eilman, D. J., Ereer, S. T., Hamlin, R., Hol, W. G. J., Kisliuk, R. L., Pastore, E. J., Plante, L. T., Xuong, N., & Kraut, J. (1978) *J. Biol. Chem. 253*, 6946–6954.

Nixon, P. F., & Blakley, R. L. (1968) *J. Biol. Chem. 243*, 4722–4731.

Norton, R. S., Clouse, A. O., Addleman, R., & Allerhand, A. (1977) *J. Am. Chem. Soc. 99*, 79–83.
Oldfield, E., & Allerhand, A. (1975a) *J. Am. Chem. Soc. 97*, 221–224.
Oldfield, E., & Allerhand, A. (1975b) *J. Biol. Chem. 250*, 6403–6407.
Oldfield, E., Norton, R. S., & Allerhand, A. (1975) *J. Biol. Chem. 250*, 6381–6402.
Perkins, S. J., & Dwek, R. A. (1980) *Biochemistry 19*, 245–258.
Seidman, K., & Maciel, G. E. (1977) *J. Am. Chem. Soc. 99*, 3254–3263.
Spiess, H. W. (1978) *NMR: Basic Princ. Prog. 15*, 55–214.
Sturtevant, J. M. (1977) *Proc. Natl. Acad. Sci. U.S.A. 74*, 2236–2240.
Tran-Dinh, S., Fermandjian, S., Sala, E., Mermet-Bouvier, R., Cohen, M., & Fromageot, P. (1974) *J. Am. Chem. Soc. 96*, 1484–1493.
Wessels, P. L., Feeney, J., Gregory, H., & Gormley, J. J. (1973) *J. Chem. Soc., Perkin Trans. 2*, 1691–1698.
Woolfenden, W. R., & Grant, D. M. (1966) *J. Am. Chem. Soc. 88*, 1496–1502.
Wüthrich, K., & Wagner, G. (1975) *FEBS Lett. 50*, 265–268.

Phosphoenolpyruvate-Dependent Phosphotransferase System of *Staphylococcus aureus*: ^{1}H Nuclear Magnetic Resonance Studies on Phosphorylated and Unphosphorylated Factor III^{lac} and Its Interaction with the Phosphocarrier Protein HPr†

H. R. Kalbitzer,* J. Deutscher, W. Hengstenberg, and P. Rösch

ABSTRACT: The trimeric phosphocarrier protein factor III specific for galactosides was investigated by ^{1}H NMR spectroscopy. The protomer contains four histidyl residues with acidic pK values in the range 5.6–6.2. One of the histidyl residues, His-B, carries the phosphoryl group. The pK value of His-B increases from 6.0 to 8.6 upon phosphorylation. To determine the position of the phosphoryl group with respect to the nitrogens required the isolation of a peptide T-2 containing the phosphorylated active-center histidine and one of the other histidines. The pK value and the chemical shift of the phosphopeptide clearly indicated the phosphorus to be bound to the N-3 atom of the imidazole ring. The temperature dependence of the factor III spectrum demonstrates multiple conformations which exchange rapidly on the NMR time scale. Titration of factor III with HPr protein showed an upfield shift of the active-center histidine, indicating complex formation between both proteins. Phosphorylation of both proteins abolished the interaction, which is plausible from mechanistic considerations.

In 1964, Kundig and co-workers discovered that in *Escherichia coli* carbohydrates are transported across the cell membrane by the phosphoenolpyruvate-dependent phosphotransferase system (PTS)[1] (Kundig et al., 1964). In subsequent years, this transport system has been found in many different microorganisms (Hengstenberg, 1977), e.g., in *Staphylococcus aureus*. The lactose-specific PTS of *S. aureus* may be described by eq 1–4. Both proteins involved in reaction 3 can be obtained in pure form and have a relatively low molecular weight of 7685 (HPr protein) (Beyreuther et al., 1977) and 33 000 (factor III) (Hays et al., 1973), respectively. It has been shown by NMR methods that HPr protein has the phosphoryl group covalently bound to nitrogen 1 of the single histidyl residue during the phosphoryl transfer (Gassner et al., 1977). Selective nitration of the three tyrosyl residues of HPr combined with ^{1}H NMR studies gave some insight into the structure of this protein (Schmidt-Aderjan et al., 1979; Rösch et al., 1981). Factor III^{lac} is composed of three identical protomers. Each subunit can be loaded with one phosphoryl group, supposedly bound to the N-3 atom of one of the histidyl residues (Hays et al., 1973). It has been shown that phosphorylation leads to a destabilization of the trimeric structure of FIII and that phosphorylated FIII in contact with the cell membrane may dissociate in its subunits (Hengstenberg, 1977).

$$\text{PEP} + \text{enzyme I} \underset{}{\overset{Mg^{2+}}{\rightleftharpoons}} \text{P–enzyme I} + \text{pyruvate} \quad (1)$$

$$\text{P–enzyme I} + \text{HPr} \rightleftharpoons \text{P–HPr} + \text{enzyme I} \quad (2)$$

$$\text{P–HPr} + \text{factor III} \rightleftharpoons \text{P–factor III} + \text{HPr} \quad (3)$$

$$\text{P–factor III} + \text{galactoside} \underset{Mg^{2+}}{\overset{\text{enzyme II}}{\rightleftharpoons}} \text{galactoside-6-P} + \text{factor III} \quad (4)$$

In this paper, we report about the effect of phosphorylation on the structure of FIII and the interaction with the phosphocarrier protein HPr as studied by NMR methods.

† From the Departments of Molecular Physics (H.R.K.) and Biophysics (P.R.), Max-Planck-Institute for Medical Research, D-6900 Heidelberg, and Department of Microbiology (J.D. and W.H.), Ruhruniversität Bochum, D-4630 Bochum, Federal Republic of Germany. *Received February 20, 1981.*

[1] Abbreviations used: PTS, phosphoenolpyruvate-dependent phosphotransferase system; NMR, nuclear magnetic resonance; HPr, histidine-containing phosphocarrier protein; P-HPr, phosphorylated HPr protein; FIII, factor III^{lac}; P-FIII, phosphorylated FIII; DTT, dithiothreitol; PMSF, phenylmethanesulfonyl fluoride; PEP, phosphoenolpyruvate; EDTA, ethylenediaminetetraacetic acid; Tris, tris(hydroxymethyl)aminomethane.

0006-2960/81/0420-6178$01.25/0